Discover Molecules

Research

Citrus IntegroPectin: a computational insight

Valeria Butera[1] · Rosaria Ciriminna[2] · Chiara Valenza[3] · Giovanna Li Petri[2] · Giuseppe Angellotti[2] · Giampaolo Barone[1] · Francesco Meneguzzo[4] · Valentina Di Liberto[3] · Angela Bonura[5] · Mario Pagliaro[2]

Received: 6 December 2024 / Accepted: 5 March 2025
Published online: 01 April 2025

Abstract
Imparted with uniquely high and broad-scope bioactivity including antioxidant, anti-inflammatory, cardioprotective, neuroprotective, antimicrobial and anticancer properties, the IntegroPectin bioconjugate obtained from citrus processing waste via hydrodynamic cavitation (HC) was investigated via Density Functional Theory computational approach. The main flavonoids of grapefruit (naringenin), orange (hesperidin), and lemon (eriocitrin) were taken into account along with a model structure for pectin including the RG-I rhamnogalacturonan chains. Results indicate that the pectin-flavonoid conjugate formation is slightly endergonic for all three conjugates, confirming the key role of HC in opening an energy window that allows overcoming the slightly positive ΔG_{form} thanks to the energy released by the imploding cavitation bubbles.

Keywords IntegroPectin · Pectin · Citrus · Flavonoids · RG-I pectin

1 Introduction

Ubiquitous in the cell wall of the pericarp of fruits and in non-graminaceous plants, pectin is a heteropolysaccharide consisting of a galacturonic acid polymer with homogalacturonan (HG), rhamnogalacturonan-I (RG-I), rhamnogalacturonan-II (RG-II), arabinogalacturonan (AG), and xylogalacturonan (XGA) regions [1]. In detail, the polymer is made of repeating units of (1 → 4)-α-D-GalA (galactopyranosyluronic acid) residues, partly methyl-esterified at O-6 position and to a lower extent also acetyl-esterified at O-2 or O-3, interrupted by branched regions composed of (1 → 2)-α-l-rhamnose units (RG-I regions) further binding neutral sugars including galactose, arabinose, xylose, and fructose [1]. The RG-I and RG-II "hairy" regions are structurally similar in different fruit and vegetable tissues [2].

Commercially sourced from lemon, orange and apple peel via prolonged acid hydrolysis using mineral acid in hot water followed by concentration via vacuum evaporation and alcohol precipitation [3], pectin is the most valued food hydrocolloid [4]. Though isolated in highly degraded form having lost most of its RG-I and RG-II regions during the hydrolytic

Supplementary Information The online version contains supplementary material available at https://doi.org/10.1007/s44345-025-00013-z.

✉ Valeria Butera, valeria.butera@unipa.it; ✉ Rosaria Ciriminna, rosaria.ciriminna@cnr.it; ✉ Mario Pagliaro, mario.pagliaro@cnr.it | [1]Dipartimento di Scienze e Tecnologie Biologiche, Chimiche e Farmaceutiche, Università di Palermo, v.Le delle Scienze Ed.17, 90128 Palermo, Italy. [2]Istituto per lo Studio dei Materiali Nanostrutturati, CNR, via U. La Malfa 153, 90146 Palermo, Italy. [3]Dipartimento di Biomedicina, Neuroscienze e Diagnostica Avanzata, Università di Palermo, C.So Tukory 129, 90134 Palermo, Italy. [4]Institute of Bioeconomy, National Research Council of Italy, Via Madonna del Piano 10, 50019 Firenze, Sesto Fiorentino, Italy. [5]Istituto di Farmacologia Traslazionale, CNR, via U. La Malfa 153, 90146 Palermo, Italy.

extraction with mineral acid [5], the polysaccharide has broad-scope bioactivity [6]. So numerous are its health benefits that pectin has been called "a universal medicine" [7].

Plentiful research efforts have been devoted in the last two decades (2003–2023) to develop new and greener pectin extraction routes [8], as well as to unlock the potential of the green extraction of bioactives from orange peel waste [9]. Amid said routes, one approach consists in replacing mineral acid with citric acid and use pulsed ultrasounds to promote the extraction of pectin from dried pomelo peel, with significantly higher pectin yield and degree of esterification (DE, the percentage of methyl-esterified carboxylic groups) compared to the conventional extraction with hot acid water [10]. Two alternative approaches which do not require the use of acid or peel drying, are the direct extraction of pectin from fresh citrus processing waste using microwaves [11] or cavitation (both hydrodynamic [12] and acoustic [13]) carried out in water only.

The latter extraction routes followed by lyophilization or spray-drying of the aqueous extract [14], have led to the isolation of a new pectin rich in RG-I regions, citrus flavonoids [15] and terpenes [16] concentrated at the surface named "IntegroPectin". Sourced from the main citrus fruits (lemon, orange and grapefruit), said new bioconjugates have vastly enhanced bioactivity in comparison to commercial citrus pectin [17].

In a series of biochemical and animal studies lately reviewed [17], said enhanced biological activity has been ascribed to the synergistic action of the citrus flavonoids and terpenes at the polymer surface along with the enhanced amount of RG-I regions partly preserved during the cavitation-assisted extraction conducted in water only.

Flavonoids at the outer surface of the IntegroPectin biopolymers may be partly physically adsorbed or chemically bound. Their chemical analysis indeed was conducted dissolving a sample of IntegroPectin in 50 mL of aqueous ethanol assisted by sonication [15]. However, even after extraction the yellow color of both lemon and grapefruit IntegroPectin was partly retained, indirectly pointing to chemical bonding between said flavonoids and the pectic polymer. Remarkably, Auhja and co-workers in 2019 reported that naringenin, the main flavonoid present in grapefruit peel, when reacted with pectin employing dicyclohexylcarbodiimide (to activate the carboxylic groups of pectin) and dimethylaminopyridine (as a coupling agent) chemically binds to pectin GalA units through all its 3 hydroxyl groups [18].

The resulting pectin-naringenin conjugate shows significantly enhanced, antioxidant, antimicrobial and anti-cancer activity ascribed to enhanced delivery of naringenin bound to water-soluble pectin over the native biophenol.

In 2020, Kumar and co-workers carried out a molecular docking study to explain the antibacterial and anti-cancer of mulberry pectin, in which pectin was modeled as a tetramer of galacturonic acid devoid of methyl-esterified carboxylic groups (about 80% in natural native pectins) [19]. The outcomes of calculations showed that pectin binds effectively with the key enzyme receptors 1e3g (binder to the receptor site of human androgen and progesterone), 3t0c (structure of *Streptococcus mutans* MetF), 5czz (structure of *Staphylococcus aureus* Cas9), 6j7l (structure of *Pseudomonas aeruginosa* Earp), 6v40 (structure of *Salmonella typhi* TtsA), 5ibs (encoded cytoplasmic protein causing mutations and leukemia in mice), 5zsy (a protein involved in the post-transcriptional processing and also in the splicing of the mRNA), and 6ggb (causing mutation of cancer, releasing unstable protein, and targeting chaperons) in Protein Data Bank). The team concluded that mulberry pectin will be used "for the treatment of many chronic diseases" [19].

More recently, Petković Benazzouz and co-workers reported the outcomes of another molecular docking analysis aimed at evaluating the influence of the degree of esterification (methylation) of pectin on the anticancer and antimicrobial properties of pectin [20]. Pectin was modeled as a trimer of three 1 → 4)-α-D-GalA units: one in which all three units are GalA, and three other structures having one, two or three methylated carboxyl groups. Two sets of biomolecules were used: one including enzymes responsible for anticancer activity, and one including those for antimicrobial activity.

In this study, we modeled IntegroPectin as a dimer in which one galacturonic unit is linked to a rhamnose molecule representing the RG-I hairy regions thereby forming the "Pec-RGI" structure to investigate via density functional theory (DFT) calculations whether the formation of the conjugate pectin-flavonoid is energetically favored. For each citrus fruit IntegroPectin the most abundant flavonoid (naringenin for grapefruit, hesperidin for orange, eriocitrin for lemon) was selected. The results shed further light on the structure of this phytocomplex holding significant nutraceutical and therapeutic potential.

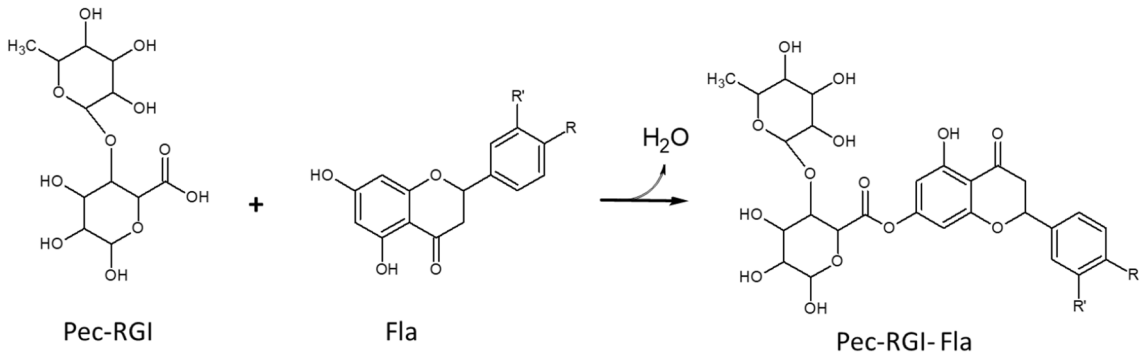

Scheme 1. Esterification reaction leading to the formation of the pectin-flavonoid conjugate

2 Methodology

2.1 Computational details and reproducibility of the results

Computational modeling is a powerful tool for the investigation of molecular and crystal structures. Among all the computational approaches, those based on DFT calculations, both at molecular and periodic boundary conditions level, are the most commonly used due to the optimal compromise between accuracy and computational cost in comparison with the alternative semi-empirical methods [21, 22] and wavefunction-theory-based approaches [23, 24] A detailed analysis of the different DFT-based computational methods along with a rigorous introduction about this widely used theory has been published lately [25].

All the calculations have been performed using GAUSSIAN 16 code [26] at the B3LYP level of theory [27]. Suitable for different kind of molecular systems [28], including reaction mechanisms [29, 30] and structure properties [31], the selected functional has been widely used. The standard 6–31 + G** basis sets of Pople and co-workers were employed for the all the atoms. Frequency calculations were carried out to check the nature of the stationary points as minima, and to determine the Gibbs corrections, which were included in the free energies discussed in this work. In order to take into account the solvent effect, the structures were fully optimized in water using the implicit polarizable continuum model (PCM) [32] as implemented in Gaussian16. This model uses the integral equation formalism variant, and it creates the solute cavity via a set of overlapping spheres.

The selected model to simulate the IntegroPectin consists of a pectin dimer in which one galacturonic unit is linked to a rhamnose unit, thus forming the Pec-RGI structure shown in Scheme 1. To increase data transparency and reproducibility of the research process and verify the validity of the results, we provide the atomic coordinates of all the optimized structures in the Supporting Information.

Formation of the pectin-flavonoid conjugate (Pec-RGI-Fla) occurs by esterification reaction, which involves the interaction of the COOH functionality of the pectin with the OH group of the flavonoid, and the consequent release of a water molecule (Scheme 1). The difference in the chemical structures among naringenin, eriocitrin and hesperidin are the R and R' substituents on the flavonoids. The corresponding functional groups are: R = OH, R' = H in naringenin, R = OCH_3 and R' = OH in eriocitrin and R = OH and R' = OH in hesperidin.

3 Results and discussion

3.1 Computational outcomes

In order to determine the potential formation of the Pec-RGI-Fla conjugates, the corresponding ΔG_{form} have been calculated from Eq. 1:

$$\Delta G_{form} = G_{(Pec-RGI-Fla)} + G_{(H2O)} - G_{(Pec-RGI)} - G_{(Fla)} \quad (1)$$

Table 1 Calculated ΔG_{form}, for all the Pec-Fla conjugates

Compound (Conjugate)	ΔG_{form} (kcal/mol)
Pec-Nar	4.6
Pec-Hes	3.3
Pec-Eri	4.9

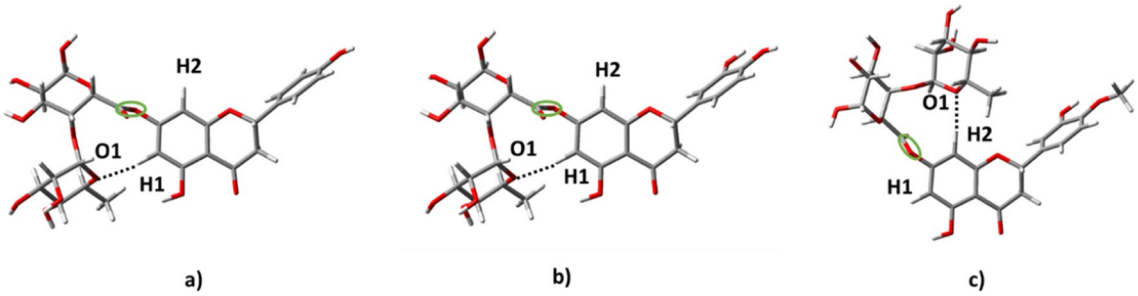

Fig. 1 Optimized structures of the pectin conjugates with naringenin (**a**), eriocitrin (**b**) and hesperidin (**c**)

where $G_{(Pec\text{-}RGI)}$, $G_{(Fla)}$ and $G_{(H2O)}$ are the calculated Gibbs energies of the isolated pectin, flavonoids and water, respectively, while $G_{(Pec\text{-}RGI\text{-}Fla)}$ is the computed Gibbs energy of the Pec-Fla conjugates. Accordingly, negative values of ΔG_{form}, indicate that the formation of the Pec-Fla conjugates is favored.

Values in Table 1 display the calculated ΔG_{form} for all the three Pec-Fla conjugates considered in this study and show that the Pec-RGI-Fla conjugates formation is endergonic for all the three conjugates. Ranging from 3.3 to 4.9 kcal/mol, said energy values are far from being prohibitive.

During the HC-based extraction using a Venturi tube [33] at low cavitation number, as in the case of the HC-based extraction of citrus IntegroPectin [12], cavitation occurs with cavitating flow structures chiefly consisting of the re-entrant jet that flows upstream in cloud cavity [34]. The large amount of energy released upon the implosion of the cavitation bubbles creating local 'hotspots' up to 5000 K and 1000 bar pressure during the natural product extraction, provides the energy required for the slightly positive ΔG_{form} identified in this study. Indeed, an esterification reaction takes place with the help of a catalyst at an elevated temperature or by a specific enzyme in nature, since ΔG_0 of a typical esterification reaction is higher than 300 kJ/mol [35].

The optimized structures of the corresponding conjugates in Fig. 1, show that for both naringenin and eriocitrin conjugates (Fig. 1a and Fig. 1b), the pectin derivates are rotated to form a hydrogen bond between the O1 oxygen of the RGI monomer of the pectin and the H1 of the flavonoid units, whose calculated distances are equal, amounting to 2.24 Å. On the other hand, Fig. 1c shows that in Pec-RGI-Hes the O1 of the RGI monomer establishes a hydrogen bond of 2.22 Å with H2 of hesperidin molecule.

The newly formed ester C—O bond (underlined in green in Fig. 1) between the pectin and flavonoid molecules has a calculated distance of 1.35 Å for all the three optimized structures. Very similar values are also calculated for the α and β dihedral angles computed for the three compounds, listed in Table 2.

These results suggest that flavonoids in citrus IntegroPectin are molecularly bound to the GalA units due to esterification reaction during the HC-based extraction of the pectic polymer. Experimental evidence for this stems from the results of the flavonoid analysis of the lemon and grapefruit IntegroPectin carried out dispersing 600 mg of pectin powder in 50 mL of EtOH/H_2O mixture (v/v, 4:1) followed by the extraction of flavonoids via sonication (150 W) for 15 min using an ultrasonic bath operating at 35 kHz [15]. A substantial amount of the IntegroPectin flavonoids was successfully extracted, but the pectin powder after flavonoid extraction retained its yellow color, though less intense, suggesting that not all flavonoids were extracted in aqueous ethanol.

Similarly, the quantitative study of the release of flavonoids from lemon and grapefruit IntegroPectin cross-linked films in buffered solution at pH 7.3 (in Tryptic Soy Broth medium) clearly show a sustained, controlled, and slow-release (up to 72 h) of flavonoids in the aqueous environment, with prolonged release from the lemon IntegroPectin film [36], which is in agreement with the higher computed Gibbs energy of the Pec-Eri conjugate found in this study. The same

Table 2 Dihedral angle values computed for the pectin conjugates with naringenin (a, R: —OH, R': —H), eriocitrin (b, R: —OCH_3, R': —OH) and hesperidin (c, R: —OH, R': —OH)

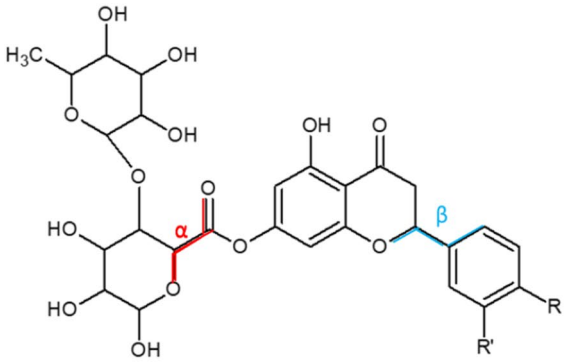

Pec-RGI- Fla

	α (°)	β (°)
Nar	178.6	126.5
Hes	-175.6	127.1
Eri	178.5	128.5

cross-linked IntegroPectin films immersed in non-buffered water quickly lower the pH thanks to the pronounced acidity of the IntegroPectin powder due, in its turn, to the low DE (and lower molecular weight) of these pectins extracted using cavitation in water only. Yet, while aqueous phase in contact with the cross-linked films readily became yellow, the grapefruit and lemon IntegroPectin films immersed in water retained their yellow color for days in the case of grapefruit IntegroPectin and for over 1 week in the case of lemon IntegroPectin.

Finally, It should be noted that the conjugate reaction formation between naringenin and the GalA units of commercial pectin through all its 3 hydroxyl groups required dicyclohexylcarbodiimide (to activate the carboxylic groups of pectin) and dimethylaminopyridine (as a coupling agent) [18]. Even with the activating and coupling agents, however, conjugate formation required prolonged reaction for 6 h at 60–65 °C (under a N_2 atmosphere) of the activated pectin dispersed in DMSO with a solution of naringenin in DMSO.

The interactions between polyphenols and polysaccharides have attracted much attention due to their excellent functional properties. A deeper understanding of the interaction between polyphenols and polysaccharides contributes to improving the stability of polyphenols in food processing, transportation, and storage processes. Numerous studies have confirmed that polyphenols and polysaccharides are mainly bound through covalent and non-covalent interactions [37]. Among them, the main non covalent binding forces of interaction between polysaccharides and polyphenols are hydrogen bonding and ion and hydrophobic interactions [38]. However, the interaction between polyphenols and polysaccharides is still influenced by the molecular structures, types, and external environmental factors.

Three mechanisms can be jointly responsible for the formation of polyphenol–cell–walls complexes. The first mechanism is non-covalent and consists of the adsorption of native and oxidized polyphenols to the cell-wall matrix, which will be detailed below [39]. Two distinct mechanisms might lead to the formation of covalent bonds by reaction with cell wall polymers of polyphenols activated either (mechanism 2) by oxidation *i.e.,* as quinones (resulting primarily from the action of polyphenol oxidase) or (mechanism 3) as carbocations, resulting from proanthocyanidin cleavage under acidic conditions [40].

As summarized by Garrido-Bañuelos, Buica, and Du Toit in 2022, polysaccharide-polyphenol interactions exist in wines and grapes [41]. The different binding mechanisms between polysaccharides and polyphenols include hydrogen bonding, hydrophobic interactions, and covalent bonds [38]. Hydrophobic interactions and hydrogen bonding mostly drive the adsorption of polyphenols by polysaccharides and can be described by various isothermal models such as Langmuir and Freundlich equations [42].

4 Conclusions

In conclusion, in this study, we modeled IntegroPectin derived via hydrodynamic or acoustic cavitation of citrus industrial processing waste from the main citrus fruits (orange, lemon and grapefruit) as a dimer in which one galacturonic unit is linked to a rhamnose molecule representing the RG-I hairy regions thereby forming the "Pec-RGI" structure to investigate via density functional theory (DFT) calculations, using B3LYP hybrid functional and the 6–31 + G* basis set, whether the formation of the conjugate pectin-flavonoid is energetically favored selecting for each citrus fruit IntegroPectin the most abundant flavonoid (naringenin for grapefruit, hesperidin for orange, eriocitrin for lemon). The formation of pectin-flavonoid complexes has also

taken into account other influencing factors, such as solvent effects as the structures were fully optimized in water using the implicit polarizable continuum model.

Even though we used a simplified model, the results of this study shed further light on the structure of this phytocomplex holding significant nutraceutical and therapeutic potential [17]. The outcomes of computation indeed indicate that the IntegroPectin-flavonoid (Pec-RGI-Fla) bioconjugate formation is endergonic for all the three bioconjugates. The energy values, however, are low ranging from 3.3 to 4.9 kcal/mol. The large amount of energy released upon the implosion of the cavitation bubbles during the natural product extraction provides the energy required for the formation of said conjugates. The outcomes of nuclear magnetic resonance experiments (NMR) from solutions of IntegroPectin will be shortly reported. Solid-state ^{13}C NMR spectra from cross-linked grapefruit and lemon IntegroPectin films, indeed, could not detect resonance peaks attributable to flavonoids [36], due their relatively low concentration relative to the main components of the films.

The limitations of the study originate from the selected models. In the framework of DFT, more extended models that better mimic the real systems, along with using computational protocols based on large basis sets and more sophisticated functionals will better mimic the real IntegroPectin phytocomplex. The accuracy of the computational predications and validations indeed heavily rely on the suitability of the selected models and protocols. However, such choices are hindered by the highly demanding computational efforts. As a consequence, the driving force for any computational study is always the balance between the reliability of the overall method and the computational costs.

In this work, we are focusing on the esterification reaction step that involves the COOH functionality of the pectin with the OH group of the flavonoid. In this regard, the esterification reaction should be only marginally influenced by the inclusion of a more extended model to mimic the IntegroPectin. In contrast, including more extended models in DFT calculations could provide higher stabilization energies due to the potential formation of additional hydrogen bonds, while molecular dynamics simulations could shed light on the rotational motions.

Remarkably, experimental validation of the computational results anticipated in this study in preprint form [43], were lately reported by Chinese scholars showing evidence that flavonoid actually binds to citrus pectin [44]. We also plan to investigate the interaction of IntegroPectin with other bioactive molecules beyond the selected flavonoids. For example, lemon, orange and red orange IntegroPectin bioconjugates from red orange and orange showing significant in vitro anticancer activity against lung cancer cells [45], contain plentiful kaempferol and p-coumaric acid.

Author contributions V. B.: Writing—Reviewing and Editing, Supervision, conceptualization, Methodology; R.C.: Conceptualization, Supervision, Methodology, Funding acquisition; Chiara Valenza: Data curation, Visualization, Investigation; G.L.P.: Data curation, Visualization, Investigation; G.A.: Data curation, Literature search; G.B.: Conceptualization, Methodology, Funding acquisition; F.M.: Data curation, Visualization, Investigation; V.D.L.: Data curation, Visualization, Investigation; A.B.: Data curation, Visualization, Investigation; M. P.: Writing—Original draft preparation, Supervision, Conceptualization, Methodology.

Data availability Atomic coordinates of all the optimized structures are provided in the Supplementary Information.

Declarations

Competing interests The authors declare no competing interests.

References

1. Ropartz D, Ralet MC. Pectin structure. In: Kontogiorgos V, editor. Pectin: Technological and Physiological Properties. Cham: Springer; 2020. p. 17–36.
2. Schols HA, Voragen AGJ. Occurrence of pectic hairy regions in various plant cell wall materials and their degradability by rhamnogalacturonase. Carbohydr Res. 1994;256:83–95. https://doi.org/10.1016/0008-6215(94)84229-9.

3. Muhidinov ZK, Khurshed I, Ikromi I, Jonmurodov AS, Nasriddinov AS, Usmanova SR, Bobokalonov JT, Strahan GD, Liu LS. Structural characterization of pectin obtained by different purification methods. Int J Biol Macromol. 2021;183:2227–37. https://doi.org/10.1016/j.ijbiomac.2021.05.094.
4. Seisun D, Zalesny N. Strides in food texture and hydrocolloids. Food Hydrocoll. 2021;117: 106575. https://doi.org/10.1016/j.foodhyd.2020.106575.
5. Wang W, Wu X, Chantapakul T, Wang D, Zhang S, Ma X, Ding T, Ye X, Liu D. Acoustic cavitation assisted extraction of pectin from waste grapefruit peels: a green two-stage approach and its general mechanism. Food Res Int. 2017;102:101–10. https://doi.org/10.1016/j.foodres.2017.09.087.
6. Ding H, Cui SW. Pectin Bioactivity. In: Kontogiorgos V, editor. Pectin: Technological and Physiological Properties. Cham: Springer; 2020.
7. Zaitseva O, Khudyakov A, Sergushkina M, Solomina O, Polezhaeva T. Pectins as a universal medicine. Fitoterapia. 2020;146: 104676. https://doi.org/10.1016/j.fitote.2020.104676.
8. Benassi L, Alessandri I, Vassalini I. Assessing green methods for pectin extraction from waste orange peels. Molecules. 2021;26:1766. https://doi.org/10.3390/molecules26061766.
9. Nayana P, Wani KM. Unlocking the green potential: sustainable extraction of bioactives from orange peel waste for environmental and health benefits. Food Measure. 2024;18:1–18. https://doi.org/10.1007/s11694-024-02779-1.
10. Wani KM, Uppaluri RVS. Continuous and pulsed ultrasound-assisted extraction of pectin from pomelo fruit peel using citric acid. Biomass Conv Bioref. 2024;14:28603–18. https://doi.org/10.1007/s13399-022-03513-x.
11. Ciriminna R, Fidalgo A, Carnaroglio D, Cravotto G, Grillo G, Tamburino A, Ilharco LM, Pagliaro M. Eco-friendly extraction of pectin and essential oils from orange and lemon peels. ACS Sust Chem Eng. 2016;4:2243–51. https://doi.org/10.1021/acssuschemeng.5b01716.
12. Meneguzzo F, Brunetti C, Fidalgo A, Ciriminna R, Delisi R, Albanese L, Zabini F, Gori A, dos Santos Nascimento LB, De Carlo A, Ferrini F, Ilharco LM, Pagliaro M. Real-scale integral valorization of waste orange peel via hydrodynamic cavitation. Processes. 2019;7:581. https://doi.org/10.3390/pr7090581.
13. Ciriminna R, Angellotti G, Li Petri G, Meneguzzo F, Riccucci C, Di Carlo G, Pagliaro M. Cavitation as a zero-waste circular economy process to convert citrus processing waste into biopolymers in high demand. J Biores Bioprod. 2024;9:486–94. https://doi.org/10.1016/j.jobab.2024.09.002.
14. Di Prima G, Scurria A, Angellotti G, Belfiore E, Pagliaro M, Meneguzzo F, De Caro V, Ciriminna R. Grapefruit IntegroPectin isolation via spray drying and via freeze drying: a comparison. Sust Chem Pharm. 2022;29: 100816. https://doi.org/10.1016/j.scp.2022.100816.
15. Scurria A, Sciortino M, Albanese L, Nuzzo D, Zabini F, Meneguzzo F, Alduina RV, Presentato A, Pagliaro M, Avellone G, Ciriminna R. Flavonoids in lemon and grapefruit IntegroPectin. ChemistryOpen. 2021;10:1055–8. https://doi.org/10.1002/open.202100223.
16. Scurria A, Sciortino M, Presentato A, Lino C, Piacenza E, Albanese L, Zabini F, Meneguzzo F, Nuzzo D, Pagliaro M, Chillura Martino DF, Alduina RV, Avellone G, Ciriminna R. Volatile compounds of lemon and grapefruit IntegroPectin. Molecules. 2021;26:51. https://doi.org/10.3390/molecules26010051.
17. Ciriminna R, Di Liberto V, Valenza C, Li Petri G, Angellotti G, Albanese L, Meneguzzo F, Pagliaro M. Citrus IntegroPectin: a multifunctional bioactive phytocomplex with large therapeutic potential. ChemRxiv. 2024. https://doi.org/10.26434/chemrxiv-2024-45v17.
18. Mundlia J, Ahuja M, Kumar P, Pillay V. Improved antioxidant, antimicrobial and anticancer activity of naringenin on conjugation with pectin. Biotech. 2019;9:312. https://doi.org/10.1007/s13205-019-1835-0.
19. Kumar RV, Srivastava D, Singh V, Kumar U, Vishvakarma VK, Singh P, Kumar D, Kumar R. Characterization, biological evaluation and molecular docking of mulberry fruit pectin. Sci Rep. 2020;10:21789. https://doi.org/10.1038/s41598-020-78086-8.
20. Martinov Nestorov J, Janjić G, Petković BM. Theoretical evaluation of pectin therapeutic potential in relation to degree of methylation. J Serb Chem Soc. 2024. https://doi.org/10.2298/JSC240422056P.
21. Yilmazer ND, Korth M. Comparison of molecular mechanics, semi-empirical quantum mechanical, and density functional theory methods for scoring protein-ligand interactions. J Phys Chem. 2013;117:8075–84. https://doi.org/10.1021/jp402719k.
22. Bosia F, Zheng P, Vaucher A, Weymuth T, Dral PO, Reiher M. Ultra-fast semi-empirical quantum chemistry for high-throughput computational campaigns with Sparrow. J Chem Phys. 2023;158:54118. https://doi.org/10.1063/5.0136404.
23. Talotta F, González L, Boggio-Pasqua M. CASPT2 potential energy curves for NO dissociation in a ruthenium nitrosyl complex. Molecules. 2020;25:2613. https://doi.org/10.3390/molecules25112613.
24. Talotta F, Heully J-L, Alary F, Dixon IM, González L, Boggio-Pasqua M. Linkage photoisomerization mechanism in a photochromic ruthenium nitrosyl complex: new insights from an MS-CASPT2 study. J Chem Theory Comput. 2017;13:6120–30. https://doi.org/10.1021/acs.jctc.7b00982.
25. Butera V. Density functional theory methods applied to homogeneous and heterogeneous catalysis: a short review and a practical user guide. Phys Chem Chem Phys. 2024;26:7950–70. https://doi.org/10.1039/d4cp00266k.
26. Frisch MJ, Trucks GW, Schlegel HB, Scuseria GE, et al. Gaussian 16, Revision C01. Wallingford (CT): Gaussian Inc; 2016.
27. Becke AD. Density-functional thermochemistry the role of exact exchange. J Chem Phys. 1993;98:5648–52. https://doi.org/10.1063/1.46491.
28. Karton A, Spackman PR. Evaluation of density functional theory for a large and diverse set of organic and inorganic equilibrium structures. J Comput Chem. 2021;42:1590–601. https://doi.org/10.1002/jcc.26698.
29. Butera V, Detz H. Hydrogenation of CO_2 to methanol by the diphosphine-ruthenium(ii) cationic complex: a DFT investigation to shed light on the decisive role of carboxylic acids as promoters. Catal Sci Technol. 2021;11:3556–67. https://doi.org/10.1039/d1cy00502b.
30. Butera V, Fukaya N, Choi JC, Sato K, Choe YK. Alkoxysilane production from silica and dimethylcarbonate catalyzed by alkali bases: a quantum chemical investigation of the reaction mechanism. Inorganica Chim Acta. 2018;482:70–6. https://doi.org/10.1016/j.ica.2018.05.036.
31. Butera V, Tanabe Y, Shinke Y, Miyazawa T, Fujitani T, Kayanuma M, Choe YK. Mechanistic investigation on ethanol-to-butadiene conversion reaction over metal oxide clusters. Int J Quantum Chem. 2021;121: e26494. https://doi.org/10.1002/qua.26494.
32. Mennucci B. Polarizable continuum model. WIREs Comput Mol Sci. 2012;2:386–404. https://doi.org/10.1002/wcms.1086.
33. Simpson A, Ranade VV. Modeling hydrodynamic cavitation in venturi: influence of Venturi configuration on inception and extent of cavitation. AIChE J. 2019;65:421–33. https://doi.org/10.1002/aic.16411.

34. Ge M, Zhang G, Petkovšek M, Long K, Coutier-Delgosha O. Intensity and regimes changing of hydrodynamic cavitation considering temperature effects. J Clean Prod. 2022;338: 130470. https://doi.org/10.1016/j.jclepro.2022.130470.
35. do Carmo FR, Evangelista NS, Fernandes FAN, de SantAna HB. Evaluation of optimal methods for critical properties and acentric factor of biodiesel compounds with their application on Soave–Redlich–Kwong and Peng-Robinson equations of state. J Chem Eng Data. 2015;60:3358–81. https://doi.org/10.1021/acs.jced.5b00638.
36. Piacenza E, Presentato A, Alduina R, Scurria A, Pagliaro M, Albanese L, Meneguzzo F, Ciriminna R, Chillura Martino DF. Cross-linked natural IntegroPectin films from *Citrus* biowaste with intrinsic antimicrobial activity. Cellulose. 2022;29:5779–802. https://doi.org/10.1007/s10570-022-04627-1.
37. Siemińska-Kuczer A, Szymańska-Chargot M, Zdunek A. Recent advances in interactions between polyphenols and plant cell wall polysaccharides as studied using an adsorption technique. Food Chem. 2022;373: 131487. https://doi.org/10.1016/j.foodchem.2021.131487.
38. Xue H, Du X, Fang S, Gao H, Xie K, Wang Y, Tan J. The interaction of polyphenols-polysaccharides and their applications: a review. Int J Biol Macromol. 2024;278: 134594. https://doi.org/10.1016/j.ijbiomac.2024.134594.
39. Renard CM, Watrelot AA, Le Bourvellec C. Interactions between polyphenols and polysaccharides: mechanisms and consequences in food processing and digestion. Tr Food Sci Technol. 2017;60:43–51. https://doi.org/10.1016/j.tifs.2016.10.022.
40. Beart JE, Lilley TH, Haslam E. Plant polyphenols—secondary metabolism and chemical defence: some observations. Phytochemistry. 1985;24:33–8. https://doi.org/10.1016/S0031-9422(00)80802-X.
41. Garrido-Bañuelos G, Buica A, du Toit W. Relationship between anthocyanins, proanthocyanidins, and cell wall polysaccharides in grapes and red wines. a current state-of-art review. Crit Rev Food Sci Nutr. 2022;62:7743–59. https://doi.org/10.1080/10408398.2021.1918056.
42. Liang J, Li H, Han M, Gao Z. Polysaccharide-polyphenol interactions: a comprehensive review from food processing to digestion and metabolism. Crit Rev Food Sci Nutr. 2024. https://doi.org/10.1080/10408398.2024.2368055.
43. Butera V, Ciriminna R, Valenza C, Li Petri G, Angellotti G, Barone G, Meneguzzo F, Di Liberto V, Bonura A, Pagliaro M. Citrus IntegroPectin: a computational insight. ChemRxiv 2024. https://doi.org/10.26434/chemrxiv-2024-hs24g.
44. Liu X, Wang F, Wang J, Liu T, Zhao C, Zheng J. Citrus flavonoid-pectin conjugates with enhanced emulsifying properties. Food Hdrocoll. 2025;159:110675. https://doi.org/10.1016/j.foodhyd.2024.110675.
45. Di Sano C, D'Anna C, Li Petri G, Angellotti G, Meneguzzo F, Ciriminna R, Pagliaro M. In vitro activity of citrus IntegroPectin against lung cancer cells. BioRxiv. 2025. https://doi.org/10.1101/2025.01.15.633201